Confinement Effects on the Thermodynamics of Protein Folding: Monte Carlo Simulations

Nitin Rathore,* Thomas A. Knotts IV,† and Juan J. de Pablo†
*Novozymes North America Inc., Franklinton, North Carolina; and †Department of Chemical and Biological Engineering, University of Wisconsin-Madison, Madison, Wisconsin

ABSTRACT The effects of chaperonin-like cage-induced confinement on protein stability have been studied for molecules of varying sizes and topologies. Minimalist models based on Gō-like interactions are employed for the proteins, and density-of-states-based Monte Carlo simulations are performed to accurately characterize the thermodynamic transitions. This method permits efficient sampling of conformational space and yields precise estimates of free energy and entropic changes associated with protein folding. We find that confinement-driven stabilization is not only dependent on protein size and cage radius, but also on the specific topology. The choice of the confining potential is also shown to have an effect on the observed stabilization and the scaling behavior of the stabilization with respect to the cage size.

INTRODUCTION

The cellular environment in which a protein folds and performs its functions is crowded with several biological molecules including lipids, carbohydrates, and other proteins. Most of the experimental, theoretical, and computational studies on protein folding, however, have relied on studying proteins in the infinitely dilute limit. This idealized dilute environment is different from that inside the cell, even if the specific interactions between the protein and the surroundings are minimal. The geometrical restrictions imposed by the neighboring molecules can have an appreciable impact on protein structure, merely by virtue of their excluded volume. Nature, in fact, utilizes such phenomena to its advantage. For example, the effects of confinement on protein folding are relevant to the functioning of chaperonin molecules. The recognition of a protein molecule by chaperonins, followed by its encapsulation in the chaperonin cage, is an important step in the folding pathway of several proteins. As a result of the aforementioned observations, folding under confinement is emerging as an active area of research. Several recent studies that include experimental (1–4), theoretical (5–7), and computational (8–13) work have been conducted to understand this phenomenon.

Eggers and Valentine (1) showed experimentally that confinement often leads to protein stabilization. For the specific case of α-lactalbumin encapsulated in a silica matrix, they found that the melting temperature increases by $\sim$30°C. Other experimental studies (3,4) also demonstrated the enhancement of protein stability in confined environments and advocated the use of nanoporous matrices for applications involving immobilized enzymes. Theoretical studies performed by Zhou and Dill (5,6) attributed this stabilization to a reduction of the entropy of the unfolded state. Based on concepts of statistical mechanics and polymer physics, they discussed how confinement enhances protein stability and folding rates. Recently, several computational groups (9–13) have also addressed this problem through the use of minimalistic models and molecular dynamics simulations. Thirumalai and co-workers (9) employed an off-lattice Gō model of a β-hairpin in a soft repulsive spherical cavity and reported a nonmonotonic dependence of the folding rate on the cavity radius. Takagi et al. (10) reported protein stabilization in a cylindrical cage and, based on the results of simulations, identified a scaling law that describes the increase in melting temperature of their simulated proteins.

Most of these computational studies have relied on the use of molecular dynamics techniques to simulate proteins in the bulk (no confinement) and inside a cage. Proteins, however, exhibit rough free energy landscapes (14,15), and canonical sampling below the melting temperature of the protein may not be sufficient to visit all the underlying minima. To overcome this limitation, several molecular dynamics simulations could be performed over a wide range of temperature, and the data could be combined using a weighted histogram approach (16); however, the statistical error associated with the tails of the sampled distributions is usually large and can propagate when data from simulations at different temperatures are merged. In this article, we use density-of-states-based (17–19) Monte Carlo methods to study proteins in the bulk and in confined environments. These methods, which rely upon uniform sampling of energy space, can yield thermodynamic data over the entire temperature range of interest and have been shown to overcome large free energy barriers. Using a Gō-like model (20), we report findings for four different proteins of various sizes and topologies. Results are presented in the form of confinement effects on the specific heat, the free energy, and the entropy of the proteins. It is shown that confinement effects on stability are protein-specific

Submitted July 20, 2005, and accepted for publication November 21, 2005.

Address reprint requests to Juan J. de Pablo, 1415 Engineering Dr., Madison, WI 53706. Tel.: 608-262-7727; Fax: 608-262-5434, Email: depablo@engr.wisc.edu.

0006-3495/06/03/1767/07 $2.00

doi: 10.1529/biophysj.105.071076

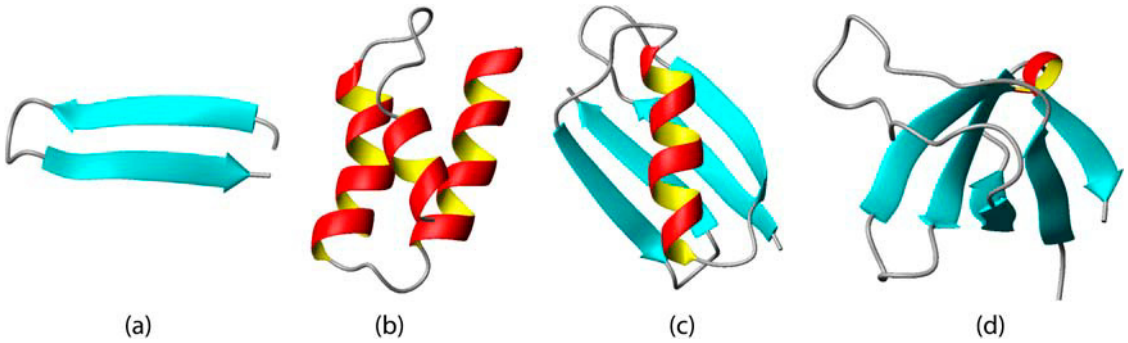

FIGURE 1 Cartoon representation of different proteins used in this study: (*a*) β-hairpin, (*b*) Protein A, (*c*) Protein G, and (*d*) SH3.

and do not always follow universal scaling as reported previously (10). For certain confining environments, individual proteins do exhibit a power-law dependence, but the relationship is different for each molecule. In other cases, the increase in stability upon confinement interestingly demonstrates nonmonotonic behavior.

MODEL AND METHODS

Protein

Four different proteins are used in this work: Protein A (1BDD), β-hairpin (16 residue fragment of 1GB1), Protein G (2GB1), and SH3 (1SRL). A schematic representation of these model proteins is given in Fig. 1.

These proteins are modeled using a coarse grain, Gō-like (20) approach. Such models and their variants have been used to investigate several kinetic and thermodynamic properties of various proteins (21–28). They have also been used to examine the effects of confinement on protein stability (9,10). Though minimalist in nature, these models have been shown to be in qualitative, and sometimes quantitative, agreement with experimental observations (10,25,29). In a Gō model, native interactions are defined by introducing an energetic bias toward the native structure. The particular implementation employed in this study is that of Hoang and Cieplak (21). We model the peptide with a bead and spring representation, with the beads placed at the C_α positions obtained from the Protein Data Bank. The interaction potential consists of the sum of the backbone potential, native interactions, and repulsive nonnative interactions. For proteins under confinement, a confining potential is added to the above mentioned interaction energy.

Confining potential

Two different potentials (9,11,12) are employed in this work (see Fig. 2). The first (9), given by Eq. 1, assigns a short-range repulsive potential between the beads of the polypeptide chain and the surface of a confining sphere. Assuming that the monomers experience a $1/r^{12}$ repulsion from the surface of the sphere, an integration is performed over the entire spherical surface to arrive at the following cage potential, V_c^A:

$$V_c^A = 4\pi\frac{\epsilon_c R_c}{5r}\left[\left(\frac{\sigma}{R_c - r}\right)^{10} - \left(\frac{\sigma}{R_c + r}\right)^{10}\right], \qquad (1)$$

where the monomer bead is located at position $\vec{R}$, $r = |\vec{R}|$, R_c is the cage radius, $\epsilon_c = 1.25$ kcal/mol, and $\sigma = 3.8$ Å is the average distance between two successive C_α atoms. The protein feels the effect of this cage potential even when it is completely inside the cage. The effect is minimal when the confining radius R_c is large compared to the size of the protein.

The second confining potential considered here is given by Eq. 2. It was originally introduced by Shea and co-workers (12), and is based on the idea that the protein should not feel the cage potential as long as it is within the cage. To capture crowding in the cell, the protein is allowed to wander outside the cage but it feels a radially inward force whenever a monomer hops out of the cage. The potential function is given by

$$V_c^B = \frac{0.01}{R_c}\left[e^{r-R_c}(r-1) - \frac{r^2}{2}\right]. \qquad (2)$$

Fig. 3 shows the qualitative difference between each type of potential and demonstrates the diversity of models that can be obtained using two different approaches. Later, in the Results and Discussion section, we show how the use of different cage potentials can lead to different thermodynamic behavior for the confined protein. The superscripts *A* and *B* are henceforth used in this article to differentiate between the two potentials.

Density of states

The thermal stability of the peptide was probed using a density-of-states-(DOS) based method (17). Previously, this method has been applied to characterize folding transitions in coarse-grained peptides on a lattice (18) and atomistic proteins in a continuum (19,30). Here, we extend these methods to examine the effect of confinement on the stability of proteins.

The DOS method has been described previously (18,19). The key quantity obtained from these simulations is the density of states, $\Omega(U)$, which is the degeneracy of energy state U. Thermodynamic quantities of

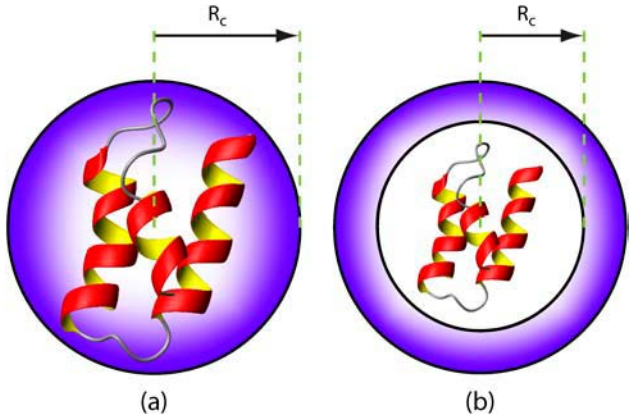

FIGURE 2 Schematic representation of Protein A in (*a*) a soft, repulsive cavity and in (*b*) a hard cavity.

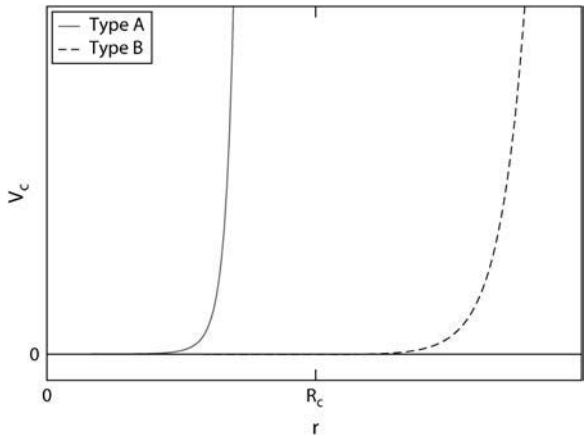

FIGURE 3 Qualitative depiction of the cavity potentials used in this study.

interest can be determined from the knowledge of the density of states. Those pertinent to this study are the internal energy $U(T)$ and the specific heat capacity $C(T)$. They are calculated according to

$$U(T) = \langle U \rangle_T = \frac{\sum U\Omega(U)e^{-\beta U}}{\sum \Omega(U)e^{-\beta U}}, \tag{3}$$

$$C(T) = \frac{\langle U^2 \rangle_T - \langle U \rangle_T^2}{k_B T^2}. \tag{4}$$

The stability of the peptide is measured in each case by determining the heat capacity as a function of temperature using Eq. 4 and assigning the transition temperature according to the position of the peak.

Once the density of states is known, other arbitrary quantities, X, such as order parameters can be determined from

$$X(T) = \langle X \rangle_T = \frac{\sum X(U)\Omega(U)e^{-\beta U}}{\sum \Omega(U)e^{-\beta U}}. \tag{5}$$

In this work, the radius of gyration, R_g, and the fractional nativeness, Q, are calculated using Eq. 5 and are used to analyze the structure of the protein.

TABLE 1 Changes in free energy, enthalpy and entropy for different proteins subjected to confinement potential V_c^A

Protein	R_c Å	T_f K	ΔG kJ/mol	ΔH kJ/mol	$T\Delta S$ kJ/mol
	Bulk	207.6	0.00	−49.53	−49.53
Protein A	30	214.4	−1.08	−45.50	−44.42
R_g = 9.4 Å	20	227.9	−2.97	−42.41	−39.44
	17	214.9	−1.19	−35.48	−34.29
	Bulk	466.8	0.00	−26.77	−26.77
β-Hairpin	30	–	−0.79	−25.10	−24.31
R_g = 7.5 Å	17	–	−2.75	−21.51	−18.76
	14	–	−3.17	−22.22	−19.04
	Bulk	353.3	0.00	−62.00	−62.00
Protein G	40	378.3	−1.99	−51.55	−49.55
R_g = 10.6 Å	25	456.1	−4.22	−40.99	−36.77
	20	–	−7.41	−44.44	−37.02
	Bulk	378.9	0.00	−89.84	−89.84
SH3	40	385.6	−1.36	−83.12	−81.76
R_g = 10.1 Å	25	436.9	−5.88	−64.31	−58.44
	20	500.0	−10.44	−65.01	−54.57

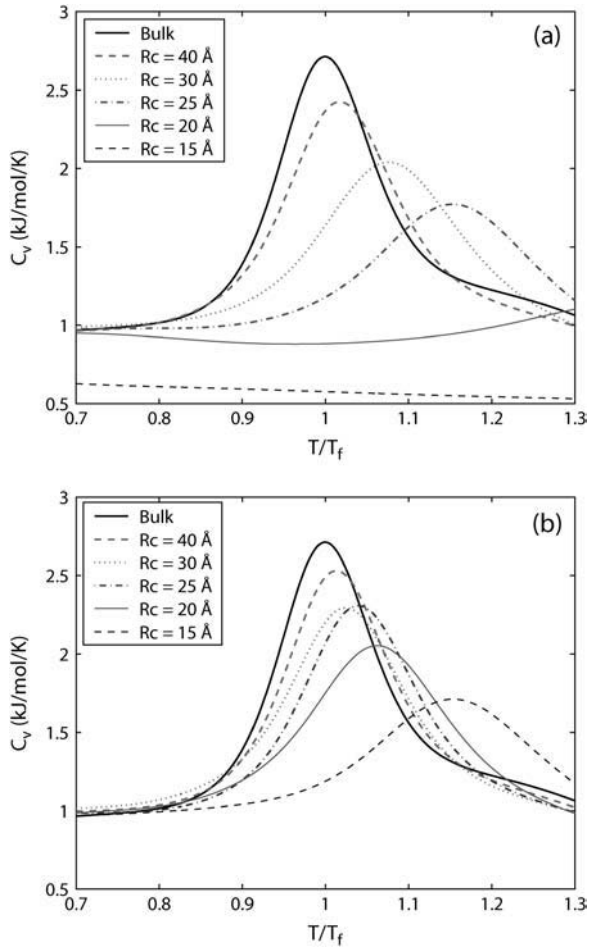

FIGURE 4 Effect of two different confining potential on the melting of protein SH3 ((*a*) V_c^A, (*b*) V_c^B).

If one adopts the view that the protein is a two-state folder, configurations sampled during the simulation can be classified into ''folded'' and ''unfolded'' ensembles based upon the number of native contacts present. The free energy of stabilization of the folded state at any temperature can then be computed from

$$\Delta G = G_{\text{folded}} - G_{\text{unfolded}} = -kT \log\left(\frac{P_f}{1-P_f}\right), \tag{6}$$

where P_f is the probability of the folded state at temperature T. The enthalpy change ΔH associated with the folding can be computed from the difference between the average potential energy of the folded and unfolded states. The entropic contribution to ΔG can then be estimated from $T\Delta S = \Delta H - \Delta G$.

It should be noted that ΔG of stabilization depends on temperature and on the definition of the folded state. Different reference states have been used in the literature. To be consistent in our treatment of different proteins, we use the fractional nativeness at the melting temperature, $Q(T_f)$, to be the threshold value for defining a folded state (a protein is considered folded if $Q > Q(T_f)$). Different proteins exhibit different amount of nativeness at the transition temperature, T_f; but such a treatment yields $\Delta G = 0$ at the transition temperature for all the proteins. This facilitates comparison of the confinement effects across several proteins in a consistent manner.

To estimate the statistical errors associated with these calculations, four independent sets of simulations, each with different random number seeds, were performed for the case of Protein A. In our simulations, different Monte Carlo moves consisting of pivot moves, random atom displacements, and

TABLE 2 Changes in free energy, enthalpy and entropy for different proteins subjected to confinement potential V_c^B

Protein	R_c Å	T_f K	ΔG kJ/mol	ΔH kJ/mol	$T\Delta S$ kJ/mol
	Bulk	207.6	0.00	−49.53	−49.53
Protein A	30	212.6	−0.85	−48.11	−47.27
$R_g = 9.4$ Å	20	215.1	−1.04	−44.24	−43.19
	17	216.9	−1.42	−44.35	−42.93
	Bulk	466.8	0.00	−26.77	−26.77
β-Hairpin	30	470.6	−0.75	−26.38	−25.63
$R_g = 7.5$ Å	17	474.3	−1.13	−25.23	−24.10
	14	–	−1.41	−23.89	−22.48
	Bulk	353.3	0.00	−62.00	−62.00
Protein G	40	367.8	−1.42	−57.14	−55.72
$R_g = 10.6$ Å	25	389.9	−2.44	−47.43	−44.99
	20	415.6	−3.19	−43.09	−39.90
	Bulk	378.9	0.00	−89.84	−89.84
SH3	40	384.1	−0.98	−85.36	−84.38
$R_g = 10.1$ Å	25	394.0	−2.53	−79.79	−77.26
	20	402.4	−3.17	−72.55	−69.38

hybrid Monte Carlo/molecular dynamics moves were utilized to sample the phase space efficiently.

RESULTS AND DISCUSSION

The effect of confinement on the thermodynamic properties of several model proteins was investigated by performing DOS simulations over a large range of temperatures. The proteins were able to sample the complete unfolded and folded states in this range. A distinct advantage of the DOS method is that it yields the specific heat as a continuous function of temperature (see Eq. 4). We computed the transition temperature for the bulk proteins and the proteins under different degrees of confinement. We also computed the free energy of stabilization (Eq. 6) and the enthalpic and entropic contributions. The results are summarized in Table 1 for cage potential V_c^A and in Table 2 for cage potential V_c^B. Earlier, Takagi et. al (10) reported that proteins with different topology and size exhibit identical behavior. We now discuss specific results for our model proteins under confinement.

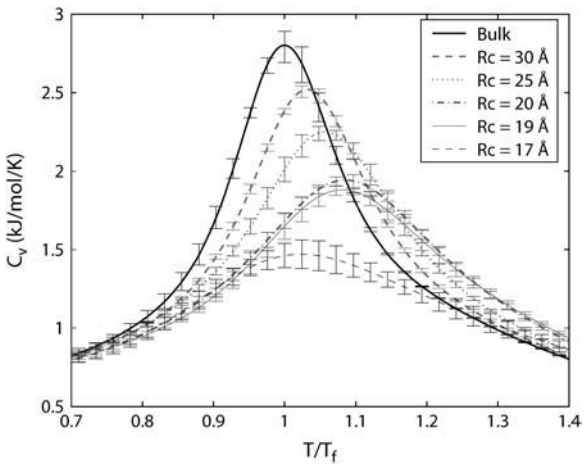

FIGURE 5 Specific heat and the associated error as a function of temperature for Protein A.

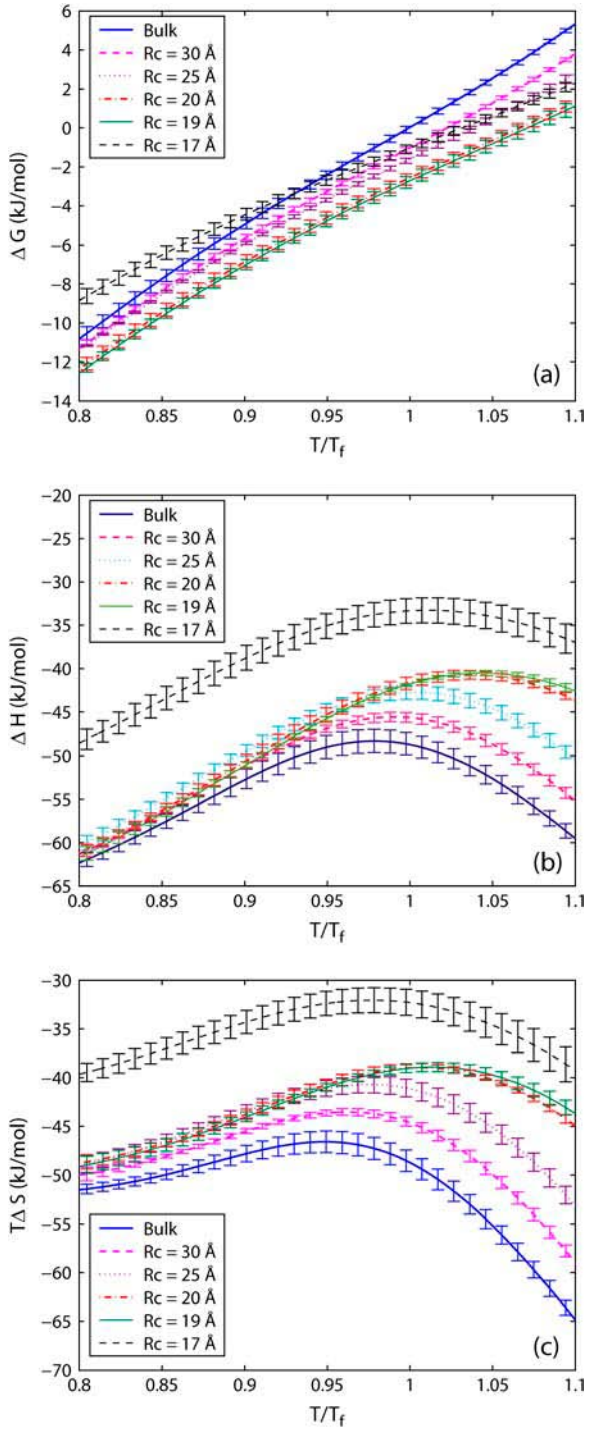

FIGURE 6 Thermodynamics of folding of Protein A: (*a*) free energy, (*b*) enthalpy, and (*c*) entropy. Statistical errors are computed based on data from four independent sets of simulations. The confined cases are for V_c^A.

SH3

SH3 is a 56 residue all β-protein. Fig. 4 shows the specific heat as a function of temperature for the two different cage potentials. The transition temperature increases as confinement radius decreases. Clearly, for the same degree of confinement, cage potential V_c^A has a more significant effect than V_c^B. This is expected from the functional form of the two potentials. Potential A has a larger effect because the protein feels it even when located completely within the cavity. The stabilization effect of confinement is also reflected in the free energy of stabilization at the melting temperature (see Tables 1 and 2). Confinement limits the conformational space available to the unfolded state and hence destabilizes the unfolded state by reducing its entropy. There is an enthalpic penalty for confining the protein but the favorable contribution of entropy dominates over the enthalpy.

Protein A

This is a 46-residue, all-helical protein that is slightly smaller than SH3. Protein A, however, exhibits a different behavior than that observed for SH3 or reported earlier for several proteins (10). Fig. 5 shows the specific heat of Protein A under different degrees of confinement defined by V_c^A. The transition temperature increases with confinement in the beginning but, in contrast to the behavior of SH3, this increment is smaller for comparable values of R_g/R_c. Upon further confinement ($R_g/R_c > 0.5$), the melting curves shift toward a lower temperature, indicating that the protein is destabilized. This demonstrates that confinement effects are protein specific. Protein A, in a cage defined by potential V_c^B, does not exhibit this reverse trend for the range of confinement radii studied here; however, the amount of stabilization is markedly smaller than that observed for other proteins.

To understand the nonmonotonic stabilization of Protein A in more detail, Fig. 6 shows the free energy, enthalpy, and entropy of folding for Protein A in the bulk and for confinement according to V_c^A. The temperature is normalized with respect to the folding temperature of the molecule in the bulk. The free energies are consistent with the specific heat curves. The lowest-melting temperature case is the peptide in the bulk, and it has the highest free energy near the melting temperature. The free energies also show the same reverse stabilization trend that was described above.

Panels b and c of Fig. 6 show the enthalpic and entropic contributions to the free energy and demonstrate that the origin of the stability of the protein under confinement is entropic in nature. For each confined case, the entropic cost of folding is less than that of its bulk counterpart. We also see that the enthalpy of folding is not as favorable for any degree of confinement as it is in the bulk. Thus, the stabilizing effects of confinement on the protein arise from two competing factors. Folding is favored entropically but hindered energetically, and since the entropic contribution is larger in magnitude, the result is an overall increased stability for confined Protein A. Moreover, Tables 1 and 2 demonstrate that this enthalpy/entropy competition extends to all the peptides in this study. We also note that similar results have been seen for Protein A when tethered to a surface (31). In this respect, a surface can be thought of as partial confinement.

The 16-residue fragment of protein 1GB1, β-hairpin, exhibits a small peak in the specific heat; changes in the transition temperature as a result of confinement are minimal (within statistical errors). ΔG, however, shows a stabilizing (Tables 1 and 2) behavior similar to that reported earlier by

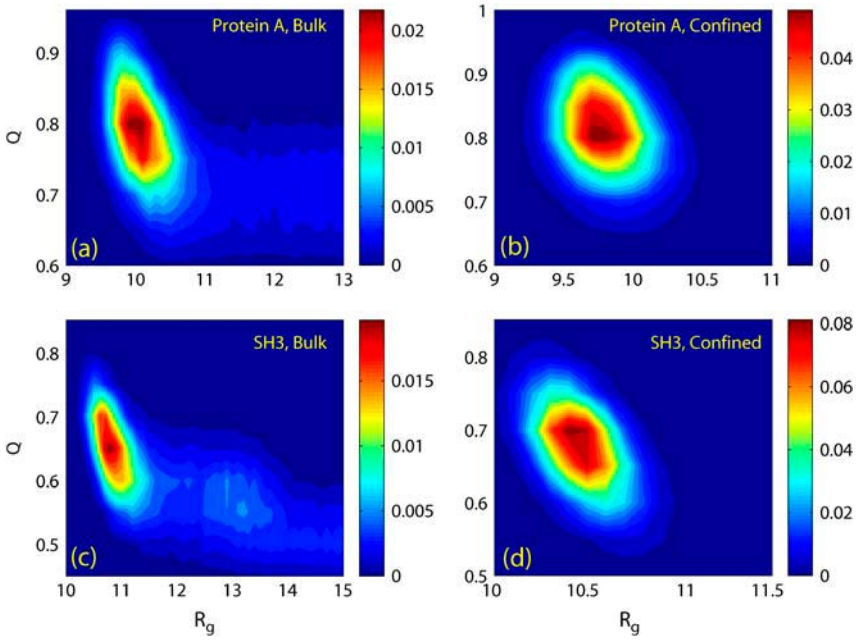

FIGURE 7 Population analysis for Protein A (a and b) and SH3 (c and d). The SH3 landscape is broader, implying that SH3 unfolded states have a larger size (R_g [=] Å) compared to those for Protein A.

Klimov et al. (9). Protein G, which has the same number of residues ($N = 56$) as SH3, shows similar large increments in its transition temperature; however, its fractional increment in T_f was larger than that of SH3. These results highlight the fact that confinement effects are dependent not just on a protein's size, but also on its overall topology and local secondary structure. Thus, we conclude that not all proteins follow a universal behavior, as originally proposed in a recent study (10), and that protein topology does play a crucial role in governing to what extent confinement will stabilize a protein.

To understand why confinement effects are markedly different in different proteins, we now examine in more detail the cases of SH3 and Protein A. Based on the analysis of C_v data and the ΔH and $T\Delta S$ contributions to ΔG, we gather that confinement does reduce the entropy of the unfolded state. This, however, comes with an enthalpic penalty, and whether confinement results in an overall stabilization of the protein or not depends upon the relative magnitude of ΔH and $T\Delta S$. Two different proteins of similar size need not show a similar balance between the enthalpic and entropic contributions to the free energy and hence will exhibit different behavior upon confinement. Fig. 7 shows population density maps as a function of radius of gyration, R_g, and fractional nativeness, Q, for Protein A (panels *a* and *b*) and SH3 (panels *c* and *d*) at their transition temperatures, in the bulk, and under confinement. As expected, the unfolded proteins visit a conformational space corresponding to larger sizes when the proteins are in the bulk than when they are confined.

A more detailed, quantitative analysis shows that for Protein A, ~50% of the population is inside the native-like basin (defined as 9.3 Å $< R_g <$ 10.4 Å); the rest of the configurations correspond to unfolded states with larger radii of gyration. Upon confinement, the unfolded state loses entropy and 99% of the population is within the native-like basin. A similar analysis of SH3 shows a much larger role of entropy. In the case of bulk SH3, at $T = T_f$, only 30% of the population lies in the native-like basin (10.0 Å $< R_g <$ 11.1 Å), whereas unfolded states occupy 70% of the conformational space. Therefore, when SH3 is confined, there is a larger favorable entropic contribution to the free energy than that observed in Protein A. As a result, SH3 exhibits confinement-driven stabilization to a greater extent than Protein A.

We now consider how confinement effects scale with protein size (R_g) and confinement radius (R_c). A recent simulation study (10) identified a universal scaling law of the form $(T_f - T_f^o) \sim R_c^{-3.25}$; which was reported to hold for multiple test cases. Two of these proteins, Protein G and SH3, are common to our study. Fig. 8 plots the fractional increment in the melting temperature as a function of the ratio of protein size and cavity radius. For the case of potential V_c^A, Protein A exhibits a nonmonotonic behavior. This potential is different from that used by Takada and co-workers. Potential V_c^B, however, is similar to theirs and we do see (Fig. 8 *b*) that the three proteins follow a scaling law. The scaling exponent ν, however, is different for each protein. The scaling does not appear to be universal. We believe, based on results for potential V_c^A ($\nu \sim 3$ for Protein G and ~4 for SH3), that ν is governed by the effective cage size imposed by the confining potential. For the same value of confining radius, R_c, potential V_c^A yields an effective pore size smaller than that of potential V_c^B, and hence the latter exhibits a smaller value of ν.

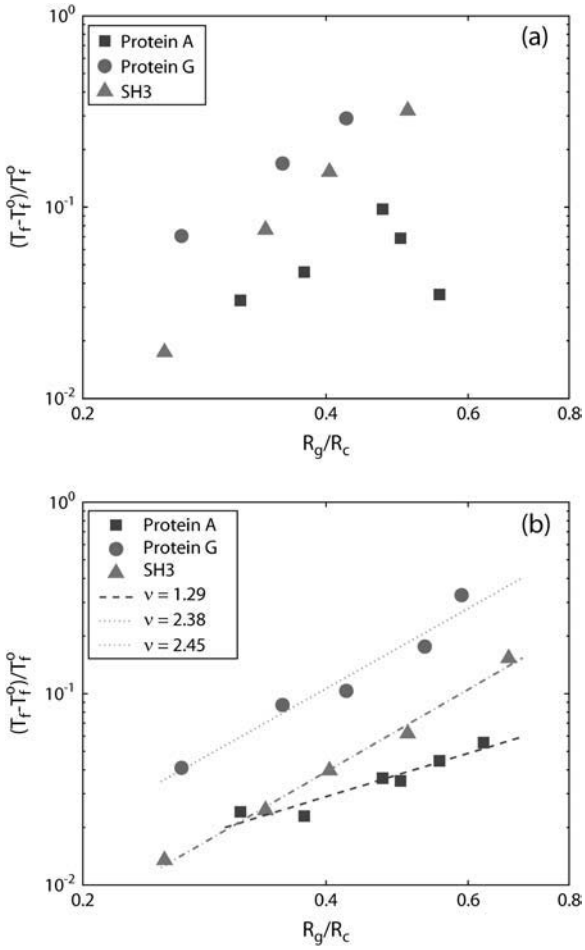

FIGURE 8 Fractional increment in melting temperatures plotted against R_g/R_c for the two confinement cases: (*a*) cage potential = V_c^A, and (*b*) cage potential = V_c^B. The lines in *b* are fits to the scaling law: $\Delta T_f/T_f^o \sim (R_g/R_c)^\nu$. Different proteins exhibit different scaling exponents.

CONCLUSIONS

We have presented a detailed analysis of confinement effects on the thermodynamics of protein folding. DOS-based Monte Carlo simulations are used to obtain precise estimates of specific heats and free energies of stabilization of folded states. Confinement reduces the entropy of the unfolded state by limiting the conformational space available to the

unfolded ensemble. It is found that proteins exhibit different stabilizing behavior under different confining potentials. Surprisingly, for the specific case of a soft repulsive potential and Protein A, it is shown that a larger degree of confinement can have a destabilizing effect. Moreover, the results for the proteins considered in this work demonstrate that confinement-driven stabilization does not always follow universal scaling as reported previously (10). It is, in fact, a result of the interplay between entropic stabilization and enthalpic destabilization. A protein's local structure and its overall topology play a crucial role in governing the relative importance of entropic and enthalpic contributions to the free energy of stabilization. The simplistic models used in this study do capture certain essential elements of the stabilizing effect of confinement. However, a more accurate treatment should take into account the crucial effect of confinement-induced changes in the water structure in the first few hydration layers surrounding the protein.

The authors are grateful to Dr. Orlando Guzmán for useful discussions and helpful suggestions. This work was supported by the University of Wisconsin Nanoscale Science and Engineering Center (N.R.) and by the National Human Genome Research Institute 5T32HG002760 (T.K.).

REFERENCES

1. Eggers, D. K., and J. S. Valentine. 2001. Molecular confinement influences protein structure and enhances thermal protein stability. *Protein Sci.* 10:250–261.
2. Campanini, B., S. Bologna, F. Cannone, G. Chirico, A. Mozzarelli, and S. Bettati. 2005. Unfolding of green fluorescent protein mut2 in wet nanoporous silica gels. *Protein Sci.* 14:1125–1133.
3. Lei, C., Y. Shin, J. Liu, and E. J. Ackerman. 2002. Entrapping enzyme in a functionalized nanoporous support. *J. Am. Chem. Soc.* 124:11242–11243.
4. Sotiropoulou, S., V. Vanvakaki, and N. A. Chaniotakis. 2005. Simulation of enzymes in nanoporous materials for biosensor applications. *Biosens. Bioelectron.* 20:1674–1679.
5. Zhou, H. X., and K. A. Dill. 2001. Stabilization of proteins in confined spaces. *Biochemistry.* 40:11289–11293.
6. Zhou, H.-X. 2004. Protein folding and binding in confined spaces and in crowded solutions. *J. Mol. Recognit.* 17:368–375.
7. Minton, A. P. 1992. Confinement as a determinant of macromolecular structure and reactivity. *Biophys. J.* 63:1090–1100.
8. Betancourt, M. R., and D. Thirumalai. 1999. Exploring the kinetic requirements for enhancement of protein folding rates in the GroEL cavity. *J. Mol. Biol.* 287:627–644.
9. Klimov, D. K., D. Newfield, and D. Thirumalai. 2002. Simulations of beta-hairpin folding confined to spherical pores using distributed computing. *Proc. Natl. Acad. Sci. USA.* 99:8019–8024.
10. Takagi, F., N. Koga, and S. Takada. 2003. How protein thermodynamics and folding mechanisms are altered by the chaperonin cage: Molecular simulations. *Proc. Natl. Acad. Sci. USA.* 100:11367–11372.
11. Baumketner, A., A. Jewett, and J. E. Shea. 2003. Effects of confinement in chaperonin assisted protein folding: Rate enhancement by decreasing the roughness of the folding energy landscape. *J. Mol. Biol.* 332:701–713.
12. Friedel, M., D. J. Sheeler, and J. E. Shea. 2003. Effects of confinement and crowding on the thermodynamics and kinetics of folding of a minimalist beta-barrel protein. *J. Chem. Phys.* 118:8106–8113.
13. Ping, G., J. Yuan, M. Vallieres, H. Dong, Z. Sun, Y. Wei, F. Y. Li, and S. H. Lin. 2003. Effect of confinement on protein folding and stability. *J. Chem. Phys.* 118:8042–8048.
14. Bryngelson, J. D., and P. G. Wolynes. 1987. Spin glasses and the statistical mechanics of protein folding. *Proc. Natl. Acad. Sci. USA.* 84:7524–7528.
15. Wolynes, P. G., J. N. Onuchic, and D. Thirumalai. 1995. Navigating the folding routes. *Science.* 267:1619–1620.
16. Kumar, S., D. Bouzida, R. H. Swendsen, P. A. Kolman, and J. M. Rosenberg. 1992. The weighted histogram analysis method for free-energy calculations on biomolecules. I. The method. *J. Comput. Chem.* 13:1011–1021.
17. Wang, F., and D. Landau. 2001. Efficient, multiple-range random walk algorithm to calculate the density of states. *Phys. Rev. Lett.* 86:2050–2053.
18. Rathore, N., and J. J. de Pablo. 2002. Monte Carlo simulation of proteins through a random walk in energy space. *J. Chem. Phys.* 116:7225–7230.
19. Rathore, N., T. A. Knotts, and J. J. de Pablo. 2003a. Density of states simulation of proteins. *J. Chem. Phys.* 118:4285–4290.
20. Abe, H., and N. Go. 1981. Noninteracting local-structures model of folding and unfolding transition in globular proteins. II. *Biopolymers.* 20:1013–1031.
21. Hoang, T. X., and M. Cieplak. 2000a. Molecular dynamics of folding of secondary structures in Gō-type models of proteins. *J. Chem. Phys.* 112:6851–6862.
22. Hoang, T. X., and M. Cieplak. 2000b. Sequencing of folding events in Gō-type proteins. *J. Chem. Phys.* 113:8319–8328.
23. Koga, N., and S. Takada. 2001. Roles of native topology and chain-length scaling in protein folding: a simulation study with a Gō-like model. *J. Mol. Biol.* 313:171–180.
24. Cieplak, M., and T. X. Hoang. 2003. Universality classes in folding times of proteins. *Biophys. J.* 84:475–488.
25. Karanicolas, J., and C. L. Brooks III. 2003. Improved Gō-like models demonstrate the robustness of protein folding mechanisms towards non-native interactions. *J. Mol. Biol.* 334:309–325.
26. Borreguero, J. M., F. Ding, S. V. Buldyrev, H. E. Stanley, and N. V. Dokholyan. 2004. Multiple folding pathways of the SH3 domain. *Biophys. J.* 87:521–533.
27. Shea, J., J. N. Onuchic, and C. L. Brooks III. 1999. Exploring the origins of topological frustration: Design of a minimally frustrated model of fragment B of protein A. *Proc. Natl. Acad. Sci. USA.* 96:12512–12517.
28. Zhou, Y., and M. Karplus. 1997. Folding thermodynamics of a model three-helix-bundle protein. *Proc. Natl. Acad. Sci. USA.* 94:14429–14432.
29. Takada, S. 1999. Gō-ing for the prediction of protein folding mechanisms. *Proc. Natl. Acad. Sci. USA.* 96:11698–11700.
30. Rathore, N., T. A. Knotts, and J. J. de Pablo. 2003b. Configurational temperature density of states simulations of proteins. *Biophys. J.* 85:3963–3968.
31. Knotts IV, T. A., N. Rathore, and J. J. de Pablo. 2005. Structure and stability of a model three-helix-bundle protein on tailored surfaces. *Proteins.* 61:385–397.